ARTHRITIS & RHEUMATOLOGY
Vol. 70, No. 10, October 2018, pp 1597–1609
DOI 10.1002/art.40535

Toll-Like Receptor 9 Deficiency Breaks Tolerance to RNA-Associated Antigens and Up-Regulates Toll-Like Receptor 7 Protein in *Sle1* Mice

Teja Celhar,[1] Hiroko Yasuga,[1] Hui Yin Lee,[1] Olga Zharkova,[1] Shubhita Tripathi,[1] Susannah I. Thornhill,[1] Hao K. Lu,[1] Bijin Au,[2] Lina H. K. Lim,[3] Thomas P. Thamboo,[3] Shizuo Akira,[4] Edward K. Wakeland,[5] John E. Connolly,[2] and Anna-Marie Fairhurst[1]

Objective. **Toll-like receptors (TLRs) 7 and 9 are important innate signaling molecules with opposing roles in the development and progression of systemic lupus erythematosus (SLE). While multiple studies support the notion of a dependency on TLR-7 for disease development, genetic ablation of TLR-9 results in severe disease with glomerulonephritis (GN) by a largely unknown mechanism. This study was undertaken to examine the suppressive role of TLR-9 in the development of severe lupus in a mouse model.**

Methods. **We crossed *Sle1* lupus-prone mice with TLR-9–deficient mice to generate *Sle1*TLR-9$^{-/-}$ mice. Mice ages 4.5–6.5 months were evaluated for severe autoimmunity by assessing splenomegaly, GN, immune cell populations, autoantibody and total Ig profiles, kidney dendritic cell (DC) function, and TLR-7 protein expression. Mice ages 8–10 weeks were used for functional B cell studies, Ig profiling, and determination of TLR-7 expression.**

Results. ***Sle1*TLR-9$^{-/-}$ mice developed severe disease similar to TLR-9–deficient *MRL* and *Nba2* models. *Sle1*TLR-9$^{-/-}$ mouse B cells produced more class-switched antibodies, and the autoantibody repertoire was skewed toward RNA-containing antigens. GN in these mice was associated with DC infiltration, and purified *Sle1*TLR-9$^{-/-}$ mouse renal DCs were more efficient at TLR-7–dependent antigen presentation and expressed higher levels of TLR-7 protein. Importantly, this increase in TLR-7 expression occurred prior to disease development, indicating a role in the initiation stages of tissue destruction.**

Conclusion. **The increase in TLR-7–reactive immune complexes, and the concomitant enhanced expression of their receptor, promotes inflammation and disease in *Sle1*TLR9$^{-/-}$ mice.**

The pattern-recognition receptors Toll-like receptor 7 (TLR-7) and TLR-9 are intracellular sensors of single-stranded RNA and double-stranded DNA (dsDNA), respectively (1). Upon binding microbial nucleic acids, signaling cascades are activated to rapidly induce an inflammatory immune response designed to clear the pathogen (1). Several mechanisms prevent the activation of TLR-7 and TLR-9 by self nucleic acids, including endosomal localization, tight regulation of their trafficking, and proteolytic processing prior to receptor activation (2,3). In systemic lupus erythematosus (SLE), however, a unique combination of self nucleic acid overload and the presence of antinuclear autoantibodies (ANAs) leads to aberrant TLR-7/9 activation (4,5). The immune complexes (ICs) formed between ANAs and their respective antigens (RNA/DNA and RNA/DNA-associated proteins) deposit in tissues where they cause chronic inflammation and ultimately lead to irreversible

Supported by core funding from Singapore Immunology Network, Agency for Science, Technology, and Research (grant to Dr. Fairhurst) and Institute of Molecular and Cell Biology, Agency for Science, Technology, and Research (grant to Dr. Connolly).

[1]Teja Celhar, PhD, Hiroko Yasuga, BSc, Hui Yin Lee, BSc, Olga Zharkova, PhD, Shubhita Tripathi, MSc, Susannah I. Thornhill, PhD, Hao K. Lu, PhD, Anna-Marie Fairhurst, PhD: Singapore Immunology Network, Agency for Science, Technology, and Research, Singapore; [2]Bijin Au, BSc, John E. Connolly, PhD: Institute of Molecular and Cell Biology, Agency for Science, Technology, and Research, Singapore; [3]Lina H. K. Lim, PhD, Thomas P. Thamboo, MD: National University Hospital, Singapore; [4]Shizuo Akira, PhD: Osaka University, Osaka, Japan; [5]Edward K. Wakeland, PhD: University of Texas Southwestern Medical Center, Dallas.

Address correspondence to Anna-Marie Fairhurst, PhD, Singapore Immunology Network, Agency for Science, Technology, and Research, 8A Biomedical Grove, #03-06 Immunos, 138648 Singapore. E-mail: annamarie_fairhurst@immunol.a-star.edu.sg.

Submitted for publication January 30, 2018; accepted in revised form April 17, 2018.

organ damage (6). Due to the similarities between TLR-7 and TLR-9 expression and shared signaling pathways, it has been predicted that the deletion of either of these receptors would be beneficial in terms of disease progression. Unexpectedly, TLR-9 deletion caused disease exacerbation in multiple models of spontaneous and induced lupus, while TLR-7 proved to be essential for disease development (7–14). These data suggest that the system is more complex than originally thought; however, the means by which TLR-9 prevents progression to severe disease are largely unknown.

Supporting the notion of their divergent in vivo roles, analysis of TLR-7/9 messenger RNA (mRNA) expression reveals a separation in regulatory mechanisms. TLR-7 is rapidly induced in human immune cells following stimulation with bacteria, viruses, lipopolysaccharide (LPS), CpG, interferon-α (IFNα), and SLE patient serum (15–19). However, TLR-9 can be induced in B cells, but is either down-regulated or unchanged in other cell types (16–20). We have previously shown this in human dendritic cell (DC) subsets, where plasmacytoid DCs (pDCs), BDCA-1+, and BDCA-3+ DCs all up-regulated TLR-7 mRNA in response to IFNα or influenza, but TLR-9 mRNA was down-regulated in pDCs (15). These differences suggest a separation of TLR-7/9 receptor roles, which might have important implications in SLE. Abundant immune complex–bound TLR-7/9 ligands and inflammatory mediators such as IFNα in SLE serum can chronically interfere with the expression of TLR-7 and TLR-9, disrupting homeostatic mechanisms to retain tolerance. Studies involving TLR-9– and/or TLR-7–deficient autoimmune mice can significantly contribute to the understating of these mechanisms, since TLRs are highly conserved in vertebrates (21) and humans and mice with lupus share the same autoantibody repertoire (22).

In this study we set out to examine the cellular mechanisms by which TLR-9 deficiency results in severe lupus nephritis. We bred B6.NZM2410-derived *Sle1* congenic mice, which develop mild autoimmune traits, with TLR-9–deficient mice to generate *Sle1*TLR-9$^{-/-}$ mice (23,24). By ages 4–6.5 months, female *Sle1*TLR9$^{-/-}$ mice developed severe autoimmunity, characterized by splenomegaly and kidney disease, similar to findings in TLR-9–deficient *MRL* and *Nba2* mice (8,10). Glomerulonephritis (GN) was associated with DC infiltration, and upon extraction, *Sle1*TLR-9$^{-/-}$ mouse renal DCs were more efficient at TLR-7–dependent antigen presentation than *Sle1* mouse controls. A comprehensive analysis of intracellular TLR-7 protein expression revealed an increase in TLR-7 expression in renal DCs and macrophages, which positively correlated with their recruitment into the kidney. Importantly, this increase in TLR-7 occurred prior to disease development, indicating a role in the initiation stages of tissue destruction. Additionally, our data show that, in the absence of TLR-9, *Sle1* mouse B cells are primed to produce more class-switched antibodies, and the autoantibody repertoire is skewed toward RNA-containing antigens. In summary, this study provides a unique understanding of the protective role TLR-9 plays in the development of autoimmunity and identifies the TLR-7 pathway as a critical instigator of disease development.

MATERIALS AND METHODS

Mice. Mice were bred at the Biomedical Resource Center (Singapore) or the University of Texas Southwestern Medical Center. The derivations of the B6.*Sle1* (*Sle1*), TLR-9$^{-/-}$, and TLR-7$^{-/-}$ mouse strains have been described previously (23–25). TLR-9$^{-/-}$ and TLR-7$^{-/-}$ mice (backcrossed to B6 more than 10 generations) and OT-II–transgenic mice were bred with *Sle1* mice (defined by the microsatellite markers D1Mit17, D1Mit113, and D1Mit202). SLE disease traits were evaluated in 4.5–6.5-month-old female mice, and functional cellular assessments were conducted using 8–10-week-old female mice. The care and use of laboratory animals conformed to the National Institutes of Health guidelines, and all experimental procedures were conducted according to an Institutional Animal Care and Use Committee–approved animal protocol.

Pathologic assessment of mouse kidneys. Proteinuria was assessed using Albustix (Bayer). Blood urea nitrogen (BUN) was assessed using a QuantiChrom Urea Assay Kit (BioAssay Systems). For evaluation of GN, mouse kidneys were fixed in formalin and embedded in paraffin, and 3-μm sections were stained with hematoxylin and eosin and with periodic acid–Schiff. Microscopic morphologic analysis was performed by an independent pathologist (TPT) according to the International Society of Nephrology/Renal Pathology Society 2003 criteria for the classification of lupus nephritis (26).

Autoantibody enzyme-linked immunosorbent assays (ELISAs). Serum autoantibodies were measured using ELISAs to detect antinucleosomes (histones and dsDNA), anti-dsDNA, anti–U1 small nuclear RNP (anti–U1 snRNP), or anti-RNA as previously described (27,28). Bound IgG was detected with alkaline phosphatase–conjugated anti-mouse IgG (Jackson ImmunoResearch) using paranitrophenyl phosphate as a substrate (Sigma). Absorbance was measured at 405/410 nm. Results are shown as arbitrary units (AU) that were calculated as absorbance at 405 nm (sample minus blank). For anti-RNA, serial dilutions of pooled serum from diseased mice were used to construct a standard curve.

ANA Luminex assay. An AtheNA Multi-Lyte ANA III Test System (Zeus Scientific) was used to measure 10 analytes (autoantibodies to SSA 52, SSA 60, SSB, Sm, RNP, Scl-70, Jo-1, centromere B, ribosomal P, and dsDNA) according to the recommendations of the manufacturer, with a goat polyclonal secondary antibody to mouse IgG heavy and light chains (Dylight 550; Abcam). Samples were run on a

Luminex 200 system using Luminex 100 IS software and analyzed using AtheNA Multi-Lyte Test System data analysis software (Zeus Scientific). Unit values reported are IU/ml for dsDNA and AU/ml for the remaining analytes.

Ig isotyping assays. Ig subtypes (IgA, IgG1, IgG2a/c, IgG2b, IgG3, and IgM) were measured using a mouse Ig isotyping bead panel (EMD Millipore), according to the recommendations of the manufacturer. This panel is designed to detect IgG2a (from BALB/c mice), which cross-reacts with IgG2c from mice on the B6 background, which we have labeled as IgG2a/c (29). Luminex plates were read on a Flexmap 3D System (Luminex) with Bio-Plex Manager version 6.0 software (Bio-Rad). IgM concentrations from cell culture supernatants were analyzed with an IgM ELISA (eBioscience) according to the recommendations of the manufacturer.

Microscopy. ANA screening was performed with NOVA Lite HEp-2 slides and the *Crithidia luciliae* indirect immunofluorescence test (CLIFT) using NOVA Lite dsDNA *Crithidia luciliae* substrate slides (both from Inova Diagnostics) according to the recommendations of the manufacturer. Sera were diluted 200-fold for HEp-2 and 40-fold for CLIFT, and a goat anti-mouse IgG DyLight 488 secondary antibody (Abcam) was used for detection. CLIFT slides were counterstained with DAPI. All images were obtained using a Zeiss LSM 800 upright confocal microscope with Zeiss Zen (Blue edition) software at 100× and 200× magnification for HEp-2 and CLIFT, respectively. HEp-2 staining patterns were evaluated by 2 independent investigators according to the International Consensus on Antinuclear Antibody Patterns. Confocal images of splenic germinal centers were obtained with an Olympus FV1000 confocal laser scanning microscope and were processed with FluoView (Olympus).

Flow cytometric analysis and cell sorting. Single-cell suspensions of the mouse spleen and kidneys were obtained as previously described with additional collagenase digestion for splenic DC analysis (30). Cells were blocked for 15 minutes in staining buffer (phosphate buffered saline with 1% fetal calf serum and 15 m*M* HEPES) containing 20% 2.4G2 hybridoma supernatant and incubated on ice for 30 minutes with the antibodies listed in Supplementary Table 1 (available on the *Arthritis & Rheumatology* web site at http://onlinelibrary.wiley.com/doi/10.1002/art.40535/abstract). When a biotin-conjugated antibody was used, cells were washed and incubated for an additional 30 minutes with a streptavidin-conjugated fluorophore. Red blood cell lysis was achieved using BD FACS lysing solution, followed by washing and resuspension in 1% paraformaldehyde. For sorting of live kidney cells, ACK lysis buffer (Lonza) was used, and cells were resuspended in staining buffer. For intracellular staining with anti–TLR-7, the BD Cytofix/Cytoperm fixation/permeabilization solution kit was used according to the recommendations of the manufacturer. Acquisition and analysis were completed using a BD Canto II, BD Fortessa, BD LSR II, or BD Symphony system, with FlowJo 10 for Windows (Tree Star). Mouse kidney cells were sorted using BD Aria II, Aria IV, and Aria V.

In vitro B cell stimulation. Mouse splenocytes stained with 5,6-carboxyfluorescein succinimidyl ester (CFSE) were resuspended in complete RPMI media, consisting of RPMI 1640 (Gibco Life Technologies) supplemented with 10% fetal bovine serum (HyClone; ThermoFisher Scientific), 15 m*M* HEPES, 100 μg/ml streptomycin, 100 units/ml penicillin, 200 μ*M* L-glutamine,10 μ*M* nonessential amino acids, 100 μ*M* sodium pyruvate (all from Gibco), and 45 μ*M* 2-mercaptoethanol (Sigma-Aldrich). They were plated at 1.5×10^6 cells/ml in round-bottomed 96-well plates in the presence of either CpG-B (ODN 1826), R848, or LPS-EB Ultrapure (all from InvivoGen) at the indicated concentrations. Activation was measured by CD69 and CD86 up-regulation at 24 hours, and proliferation at 72 hours was measured by CFSE dilution using flow cytometry. Ig subtype analysis in supernatants was measured 96 hours after stimulation.

Renal DC antigen presentation assay. Mouse kidneys cells were sorted, and cells were seeded in a 96-well plate at 1×10^4 cells per well. Where indicated, cells sorted from multiple mice were pooled to achieve sufficient cell numbers. Cells were stimulated overnight with or without 1 μg/ml R848 (InvivoGen), and then incubated with 10 μg/ml ovalbumin (Sigma-Aldrich). After 4 hours, medium was replaced with CFSE-stained *Sle1*OT-II mouse splenocytes at 2×10^5 cells per well. After 5 days of incubation, T cell proliferation was assessed by CFSE dilution.

Statistical analysis. Data were analyzed using GraphPad Prism 7.01 for Windows. Normal distribution was assessed using the Kolmogorov-Smirnov test. Gaussian data were analyzed using Student's *t*-test for 2 comparisons and ordinary one-way analysis of variance with post hoc Bonferroni adjustment for multiple comparisons for 3 or more comparisons. Nonparametric data were assessed using the Mann-Whitney test for 2 comparisons and the Kruskal-Wallis test with post hoc Dunn's multiple comparisons test for 3 or more comparisons. Where indicated, a multiple *t*-test corrected with the Holm-Sidak method was used.

RESULTS

Severe autoimmune disease in *Sle1* mice with genetic ablation of TLR-9. Cohorts of 4.5–6.5-month-old female *Sle1*TLR-$9^{-/-}$ mice and controls were analyzed for pathologic traits associated with common models of SLE. Genetic ablation of TLR-9 in *Sle1* mice resulted in splenomegaly and the expansion of all major leukocyte subsets (Figures 1A and B). There was a significant increase in CD11b+ cell numbers in *Sle1* mice versus wild-type C57BL/6J (B6) mice and in TLR-$9^{-/-}$ mice versus wild-type mice, indicating that both genetic components contribute to splenic myeloid cell expansion (Figure 1B). We detected an expansion of germinal center B cells in *Sle1*TLR-$9^{-/-}$ mice compared to *Sle1* controls, similar to observations in *Sle1b*TLR-$9^{-/-}$ and MRL/+TLR-$9^{-/-}$ mice (Figures 1C and D and Supplementary Table 2, available on the *Arthritis & Rheumatology* web site at http://onlinelibrary.wiley.com/doi/10.1002/art.40535/abstract) (9,31). We also observed increases in CD138+B220− plasma cell numbers (Supplementary Table 2) and a decreased frequency of marginal zone B cells (Supplementary Figure 1A, available on the *Arthritis & Rheumatology* web site at http://onlinelibrary.wiley.com/doi/10.1002/art.40535/abstract), which are characteristics of lupus

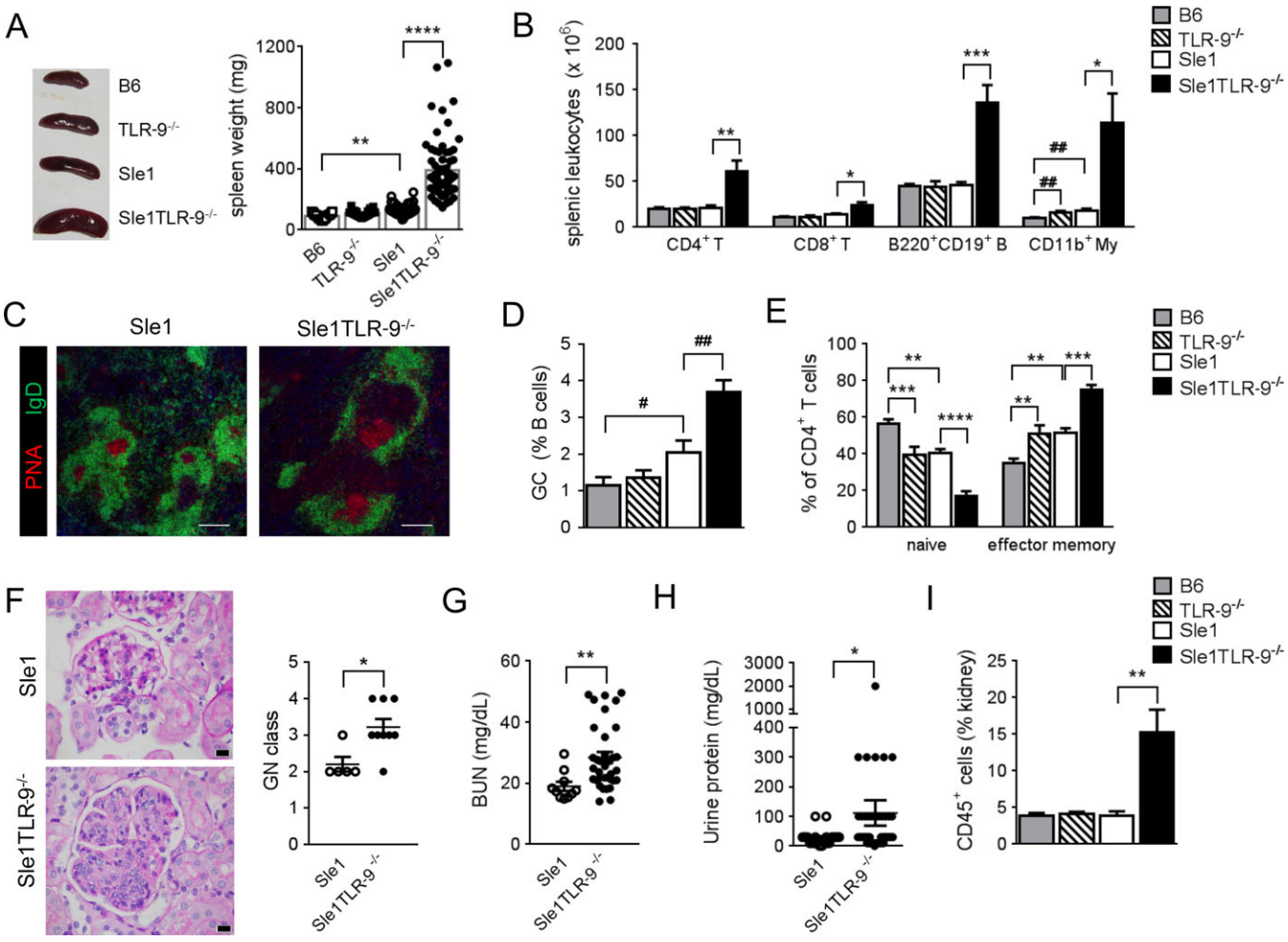

Figure 1. Severe disease in Toll-like receptor 9 (TLR-9)–deficient mice. Female B6, TLR-9$^{-/-}$, *Sle1*, and *Sle1*TLR-9$^{-/-}$ mice ages 4.5–6.5 months were analyzed for lupus disease features. **A**, Left, Representative spleens from the indicated mouse strains. Right, Cumulative splenic weights for the indicated mouse strains. Symbols represent individual mice; bars show the mean (n = 30–65 mice/group). **B**, Numbers of leukocytes of each subset in the spleens of mice of the indicated strains. My = myeloid cells. **C**, Representative images of germinal center (GC) staining in the spleens of *Sle1* and *Sle1*TLR-9$^{-/-}$ mice. PNA = peanut agglutinin. Bars = 200 μm; original magnification × 100. **D**, GC frequency measured by flow cytometric analysis of GL-7+Fas+ cells and presented as the percentage of B cells (CD19+B220+). **E**, Flow cytometric analysis of naive (CD62L^{high} CD44^{low}) and effector memory (CD62L^{low}CD44^{high}) CD4+ T cells in the spleens of mice of the indicated strains. **F**, Left, Representative photomicrographs of an *Sle1* mouse glomerulus with mild segmental mesangial proliferation and an *Sle1*TLR-9$^{-/-}$ mouse glomerulus with global endocapillary proliferation. Periodic acid–Schiff stained. Bars = 20 μm; original magnification × 600. Right, Kidney glomerulonephritis (GN) class (I–IV represented as 1–4) in *Sle1* and *Sle1*TLR-9$^{-/-}$ mice. **G** and **H**, Functional assessment of mouse kidneys. Blood urea nitrogen (BUN) (**G**) and urinary protein levels (measured by Albustix) (**H**) were determined. **I**, Infiltration of CD45+ leukocytes into the mouse kidney, assessed by flow cytometry. All flow cytometry data (in **B**, **D**, **E**, and **I**) are from 2–5 separate cohorts with a total of 6–17 mice per group. In **B**, **D**, **E**, and **I**, bars show the mean ± SEM. In **F–H**, circles represent individual mice; horizontal lines and error bars show the mean ± SEM. * = $P < 0.05$; ** = $P < 0.01$; *** = $P < 0.001$; **** = $P < 0.0001$, by one-way analysis of variance (with Bonferroni adjustment for multiple comparisons) for parametric data or Kruskal-Wallis test (with Dunn's multiple comparison test) for nonparametric data, taking into consideration all 4 groups; # = $P < 0.05$; ## = $P < 0.01$, by Student's *t*-test for parametric data or Mann-Whitney test for nonparametric data, taking into consideration only 2 groups.

models overexpressing TLR-7 (32,33). CD4+ and CD8+ T cells from *Sle1*TLR-9$^{-/-}$ mice had a more activated phenotype, with higher percentages of CD62L^{low} CD44^{high} effector memory cells and CD4+ follicular helper T cells, and increased programmed death 1 and inducible costimulator expression, consistent with observations in S*le1b*TLR-9$^{-/-}$ mice and in *Sle1* mouse models overexpressing TLR-7, such as *Sle1*Tg7 (15,31,32) (Figure 1E, Supplementary Figures 1B–D, and Supplementary Table 2).

Analysis of the splenic CD11b+ myeloid lineage revealed increases in the numbers of $Gr1^{high}$ polymorphonuclear leukocytes (PMNs) and SSC-A^{high} eosinophils in *Sle1*TLR-$9^{-/-}$ mice compared to controls (Supplementary Table 2 and Supplementary Figure 1E). $Gr1^{-/low}$ cells represented the majority of the expanding myeloid population (Supplementary Figure 1E) and were further analyzed for CD11c and major histocompatibility complex (MHC) class II expression (Supplementary Figure 1F). Conventional CD11b+ DCs (cDCs) expressing MHC class II, and a possible precursor, which lacks MHC class II, were increased; both were previously characterized in the *Sle1*Tg7 model (Supplementary Figure 1F and Supplementary Table 2) (15). Splenic F4/80+CD64+$CD11b^{intermediate}$ macrophage, CD8+ DC, and pDC numbers, but not frequencies, were increased due to increased cellularity in TLR-9–deficient *Sle1* mice (Supplementary Table 2).

Pathologic analysis confirmed that the majority of *Sle1*TLR-$9^{-/-}$ mice developed severe GN (class III–IV), characterized by segmental to global endocapillary proliferation of the glomeruli (Figure 1F). Increased serum BUN levels and urinary protein levels confirmed these findings (Figures 1G and H). GN was associated with an infiltration of CD45+ leukocytes into the mouse kidney, consisting mainly of T cells and CD11b+ myeloid cells (Figure 1I and Supplementary Table 2). CD11b+ cells were mostly $Gr1^{-/low}$, as determined previously in *Sle1*Tg7 mice (Supplementary Figure 1G) (15). B cells and pDCs comprised minor populations in the kidney infiltrates and were not significantly increased in the absence of TLR-9 (Supplementary Table 2).

TLR-9 deficiency in *Sle1* mice skews the autoantibody profile toward RNA-associated autoantigens. Previous studies have shown that TLR-9 deletion on the MRL mouse background results in a shift from homogenous nuclear to cytoplasmic ANA HEp-2 staining patterns and the loss of binding to mitotic chromatin (7–9). This coincides with lower levels of antinucleosome antibodies, but not with lower anti-dsDNA antibody titers as measured by ELISA (8). Similarly, elimination of TLR-9 decreased antinucleosome/chromatin antibodies in B6.Fas/*lpr*, Plcg2*Ali5*, and B6*Nba2* mice, while anti-dsDNA levels measured by ELISA were increased or unchanged (10,13,34).

Next, we examined the autoantibody profile in *Sle1*TLR-$9^{-/-}$ mice, using a variety of methods for clarity. Microscopy of HEp-2 cells revealed that serum autoantibodies from *Sle1*TLR-$9^{-/-}$ mice bound primarily to the cytoplasm, with some nucleolar specificity, in contrast to *Sle1* mouse sera, which bound primarily to the nucleus (Figures 2A–C). All *Sle1*TLR-$9^{-/-}$ mouse sera tested lost the ability to bind mitotic chromatin (Figures 2A and D). Consistent with this finding, the levels of antinucleosome autoantibodies were significantly decreased in *Sle1*TLR-$9^{-/-}$ mice compared to *Sle1* controls (Figure 2E). However, we detected increased levels of anti-dsDNA antibodies using an in-house ELISA and a commercial Luminex-based assay (Figure 2E and Supplementary Figure 2F, available on the *Arthritis & Rheumatology* web site at http://onlinelibrary.wiley.com/doi/10.1002/art.40535/abstract). In clinical practice, dsDNA ELISAs have shown low specificity and poor correlation with superior detection assays, such as CLIFT (35,36). We therefore tested *Sle1*TLR-$9^{-/-}$ samples from Figures 2A–D with the CLIFT assay, and 6 of 8 serum samples showed positive kinetoplast staining, confirming the presence of anti-dsDNA antibodies despite negative chromatin staining (Supplementary Figures 2A and B). High levels of anti-dsDNA as determined by anti-dsDNA ELISA did not correlate with positive CLIFT findings (Supplementary Figure 2C), confirming low specificity of the ELISA. Discrepancies between ELISA and CLIFT for anti-dsDNA measurement in TLR-$9^{-/-}$ lupus models have also been observed by other groups and are due to a number of factors, including the origin and purity of the DNA antigen used for ELISA (8,13).

The cytoplasmic HEp-2 staining pattern of *Sle1*TLR-$9^{-/-}$ mouse serum is characteristic of RNA-reactive antibodies (33,37) (Figures 2A and C), which we confirmed by anti-RNA ELISA (Figure 2E). Moreover, cytoplasmic staining intensity positively correlated with anti-RNA titers (Supplementary Figures 2D and E). Additionally, anti-snRNP autoantibody levels were higher in *Sle1*TLR-$9^{-/-}$ mice than *Sle1* mice (Figure 2E). A Luminex autoantigen assay confirmed this change and detected significant increases in several other RNA-associated autoantibodies, including anti-SSA 52 and 60, anti-SSB, anti-Sm, and anti–ribosomal P (Supplementary Figure 2F). Analyses of serum Ig levels by Luminex showed that TLR-9 deficiency resulted in significantly higher concentrations of total IgG2a/c, IgG2b, and IgM antibodies compared to *Sle1* controls, while IgA concentrations were decreased (Figure 2F).

Systemic up-regulation of TLR-7 in diseased *Sle1*TLR-$9^{-/-}$ mice. Increased TLR-7 expression leads to an augmentation in autoimmunity (15,27,33). However, it is unknown if TLR-$9^{-/-}$ mice express higher levels of TLR-7 protein. Bossaller et al recently showed an infiltration of $Ly6G^{high}Ly6C^{high}$ cells with higher levels of TLR-7 in the peritoneal cavity of TLR-$9^{-/-}$BALB/c mice with pristane-induced lupus (14). Therefore, we assessed

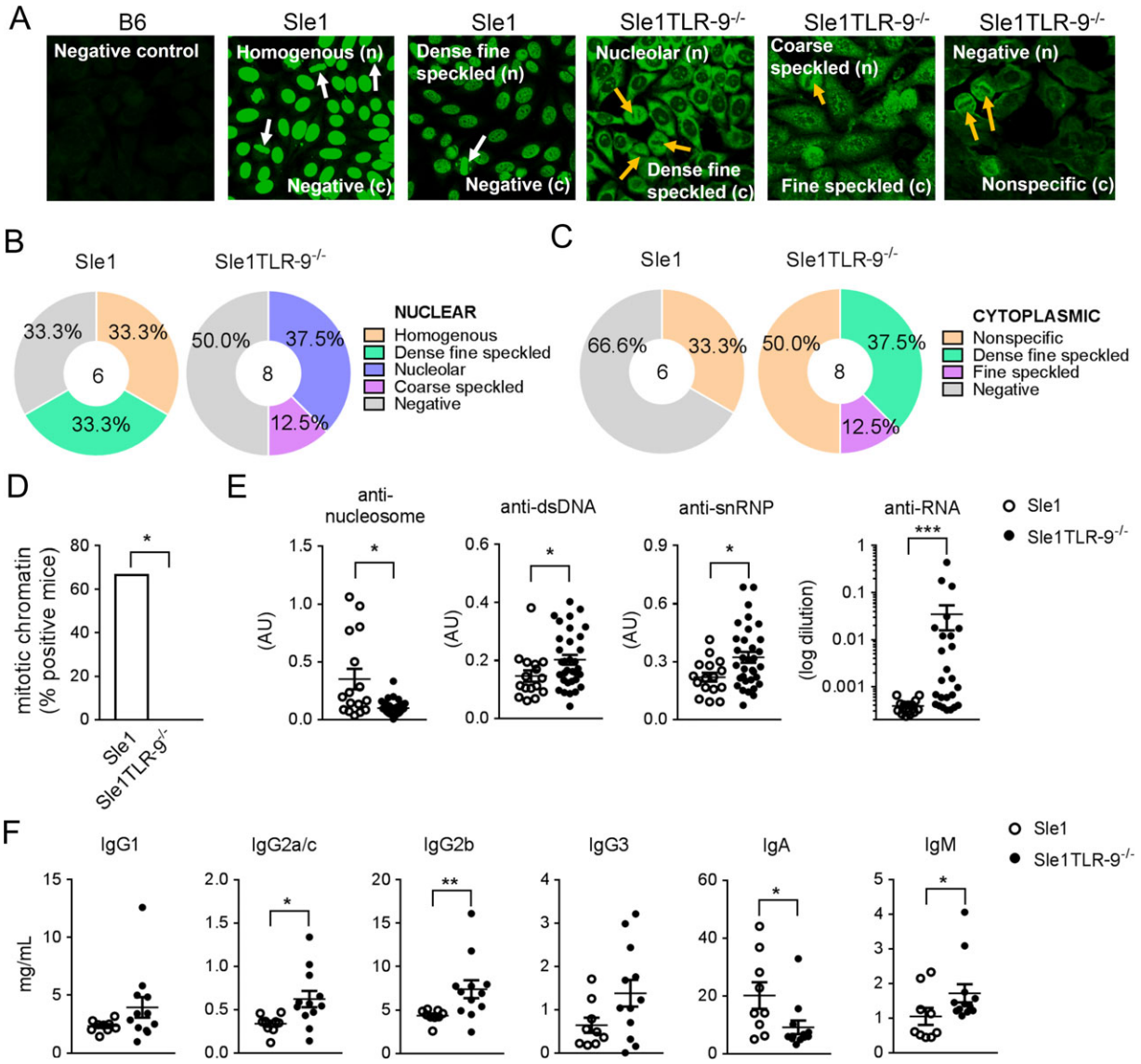

Figure 2. Toll-like receptor 9 (TLR-9) deletion in mice breaks tolerance to RNA-associated antibodies. **A**, Representative microscopy images of nuclear (**n**) and cytosolic (**c**) HEp-2 staining patterns of serum autoantibodies from B6, *Sle1*, and *Sle1*TLR-9$^{-/-}$ mice ages 4.5–6.9 months. **White arrows** show mitotic chromosome staining; **orange arrows** indicate the absence of mitotic chromosome staining. **B** and **C**, Analysis of nuclear (**B**) and cytoplasmic (**C**) staining patterns determined by HEp-2 staining and microscopy. **D**, Percentage of *Sle1* and *Sle1*TLR-9$^{-/-}$ mice with mitotic chromatin positivity. Serum for HEp-2 staining was obtained from 3 independent cohorts with a total of 6 *Sle1* mice and 8 *Sle1*TLR-9$^{-/-}$ mice. **E**, Levels of antinucleosome (double-stranded DNA [dsDNA]/histone), anti-dsDNA, anti–small nuclear RNP (anti-snRNP), and anti-RNA autoantibodies in *Sle1* and *Sle1*TLR-9$^{-/-}$ mice. Serum dilutions were 1:100 for anti-RNA and 1:200 for all other autoantibodies. AU represents absorbance at 405 nm (sample minus blank). Values for anti-RNA antibodies are represented as logarithmic values of dilutions calculated from a standard curve. **F**, Levels of IgG subtypes in sera from *Sle1* and *Sle1*TLR-9$^{-/-}$ mice analyzed by Luminex. In **E** and **F**, mouse sera were from 6 independent cohorts. Circles represent individual mice; horizontal lines and error bars show the mean ± SEM. All data presented are from 4.5–6.9-month-old mice. Parametric data were assessed by one-way analysis of variance (with Bonferroni adjustment for multiple comparisons) or Student's *t*-test, and nonparametric data were assessed by Kruskal-Wallis test (with Dunn's multiple comparison test) or Mann-Whitney test. Significance in **D** was determined by Fisher's exact test. * = $P < 0.05$; ** = $P < 0.01$; *** = $P < 0.001$.

TLR-7 expression by flow cytometry using the same antibody clone (A9410). We verified binding specificity using TLR-7–deficient B6 mice (TLR-7$^{-/-}$) and a fluorescence minus one control. Our analyses showed that TLR-7 levels were significantly higher in B cells, pDCs, CD11b+ DCs, F4/80+ macrophages, and in the CD11c+MHCII–

precursor population in *Sle1*TLR-9$^{-/-}$ mice than in *Sle1* controls (Figure 3A). TLR-7 expression positively correlated with the expansion of CD11b+ DCs and CD11c+ MHCII− subsets, but not with pDC frequencies (Figures 3B–D). TLR-7 was expressed in splenic PMNs and at significantly higher levels in TLR-9–deficient *Sle1* mice (Supplementary Figure 3A, available on the *Arthritis & Rheumatology* web site at http://onlinelibrary.wiley.com/doi/10.1002/art.40535/abstract). No differences were observed in splenic CD11b+Gr-1^{intermediate} cells, which had highly variable TLR-7 expression (Supplementary Figure 3B). As expected, TLR-7 expression was not detected in CD3+ T cells or CD8+ DCs (Supplementary Figures 3C and D).

Regulation of IgG production by TLR-9 in *Sle1* lupus-prone mice. Given the essential role of humoral immunity in the development of SLE, we assessed B cell functional responses to TLR-7 in young prediseased mice. We stimulated mouse splenocytes with the TLR-7 ligand R848 and TLR-4 ligand LPS as a TLR-7–independent

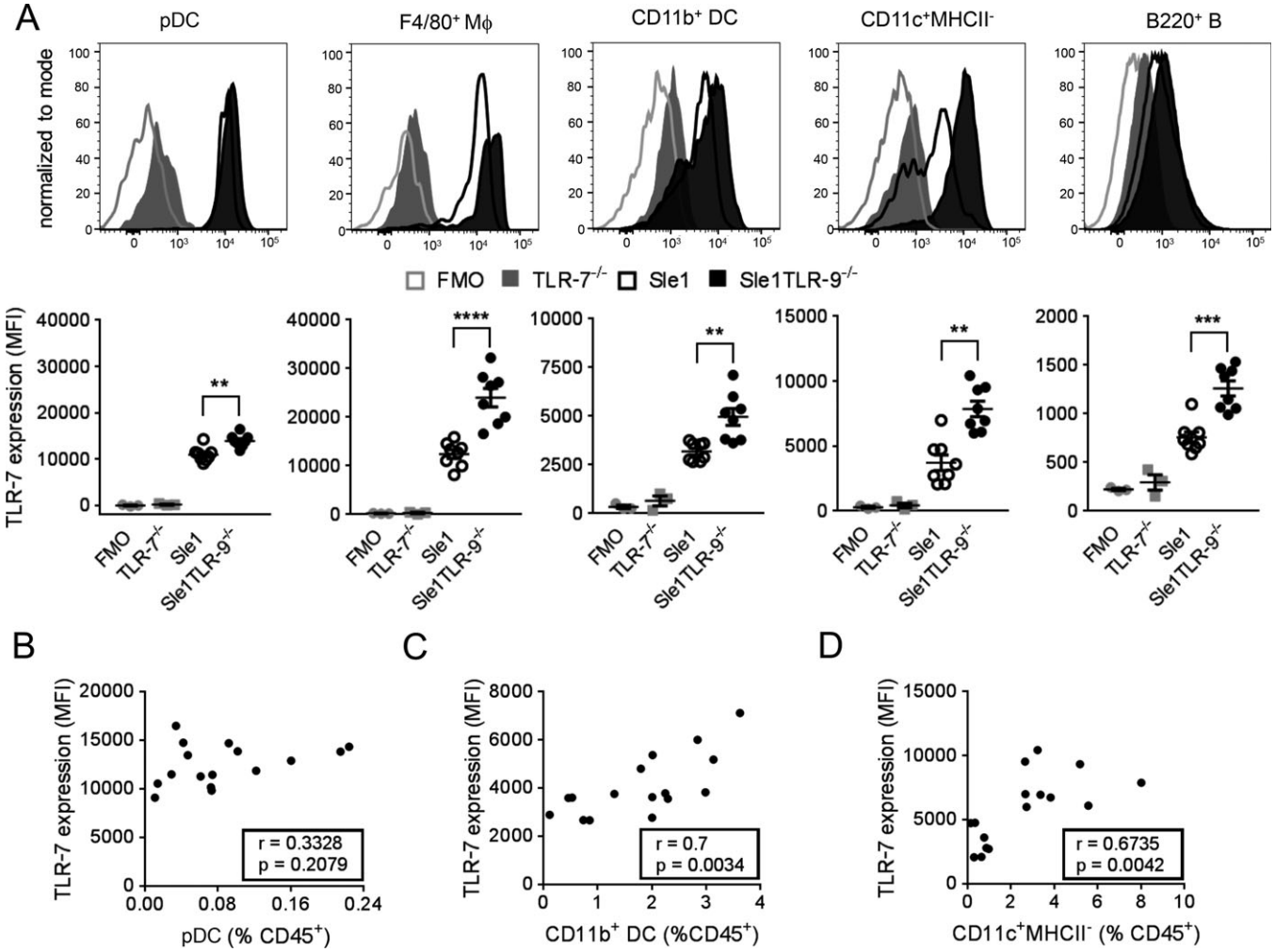

Figure 3. Regulation of Toll-like receptor 7 (TLR-7) protein expression in the mouse spleen by TLR-9 deficiency. **A**, Representative histograms (top) and median fluorescence intensity (MFI) data (bottom) for TLR-7 expression, measured by intracellular flow cytometry, in the indicated spleen cell subsets in *Sle1* and *Sle1*TLR-9$^{-/-}$ mice ages 5.7–6.4 months. Results are from 3 independent experiments each conducted with a TLR-7$^{-/-}$ and fluorescence minus one (FMO) control (n = 8 *Sle1* mice, 8 *Sle1*TLR-9$^{-/-}$ mice, 3 TLR-7$^{-/-}$ controls, and 3 FMO controls). Symbols represent individual samples; horizontal lines and error bars show the mean ± SEM. Mϕ = macrophage. **B–D**, Correlation of leukocyte expansion in *Sle1* and *Sle1*TLR-9$^{-/-}$ mouse spleens with TLR-7 expression in plasmacytoid dendritic cells (pDCs) (**B**), CD11b+ DCs (**C**), and CD11c+ major histocompatibility complex class II (MHCII)− cells (**D**). Parametric data were assessed by Student's *t*-test, and nonparametric data were assessed by Mann-Whitney test. Correlations were determined using Spearman's rank correlation for nonparametric data and Pearson's correlation for parametric data. ** = $P < 0.01$; *** = $P < 0.001$; **** = $P < 0.0001$.

signal. We used flow cytometry assays to measure B cell survival, activation, and proliferation and did not detect any significant differences between *Sle1* and *Sle1*TLR-9$^{-/-}$ mice within a wide range of R848 concentrations, in contrast to the findings of an earlier study in B6.TLR-9$^{-/-}$ CD19+B220+ mouse splenocytes (38) (Figures 4A and B and Supplementary Figures 4A–C, available on the *Arthritis & Rheumatology* web site at http://onlinelibrary.wiley.com/doi/10.1002/art.40535/abstract). Consistent with the lack of increased activation upon TLR-7 ligation, we

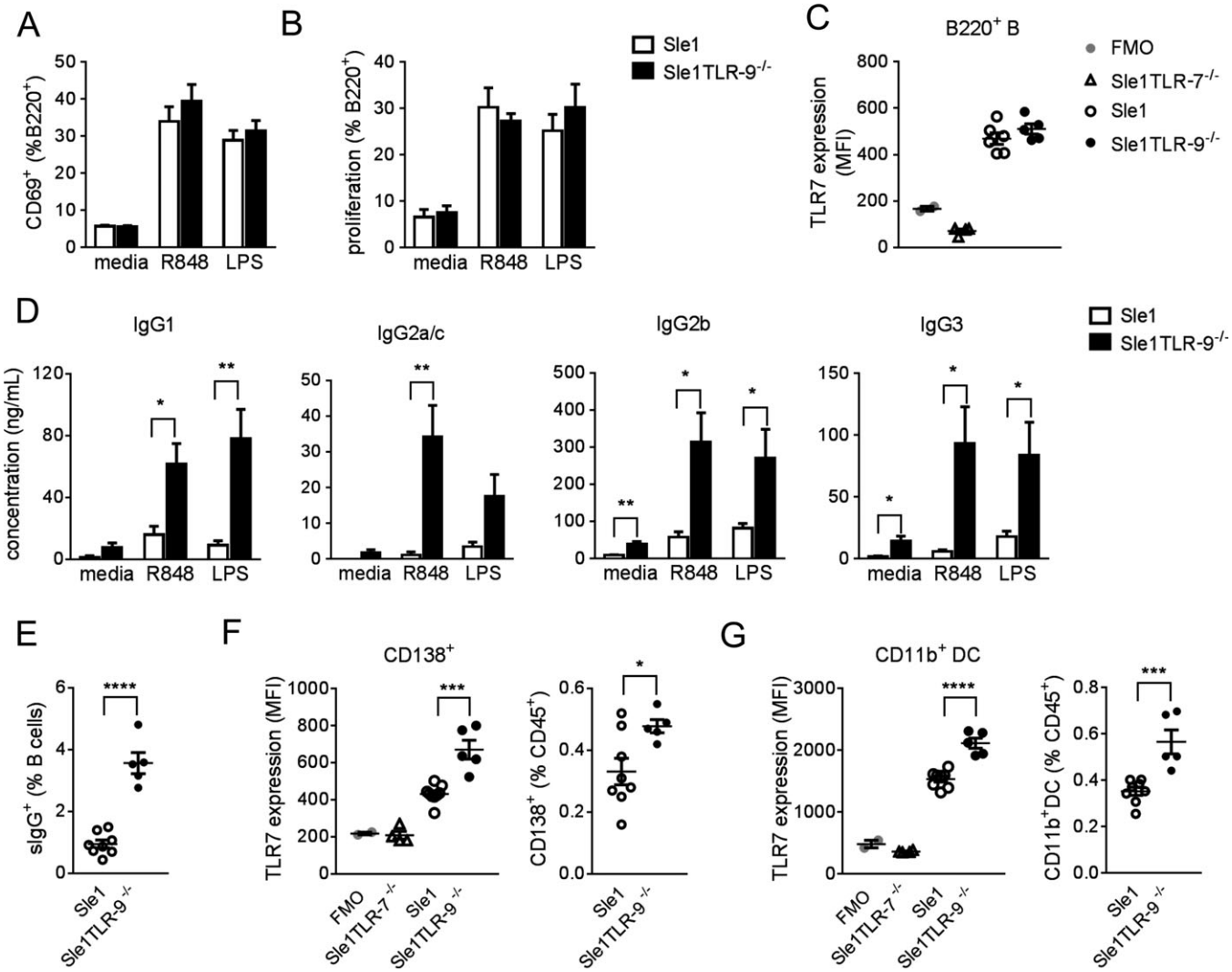

Figure 4. Regulation of antibody production by Toll-like receptor 9 (TLR-9) in *Sle1* mice. **A** and **B**, B cell (B220+) activation (**A**) and proliferation (**B**) in splenocytes from young (8–10-week-old) *Sle1* and *Sle1*TLR-9$^{-/-}$ mice that were left untreated (media), stimulated with R848 (0.01 μg/ml), or stimulated with lipopolysaccharide (LPS; 1 μg/ml). B cell activation was measured by flow cytometry after 24 hours of stimulation and is shown as the percentage of CD69+ cells. B cell proliferation was measured according to the 5,6-carboxyfluorescein succinimidyl ester dilution after 72 hours of stimulation. **C**, TLR-7 expression, measured by intracellular flow cytometry, in mouse splenic B220+ B cells. TLR-7–deficient *Sle1* mice (*Sle1*TLR-7$^{-/-}$) (n = 4) and fluorescence minus one (FMO) samples were used as negative controls. MFI = median fluorescence intensity. **D**, Levels of IgG subtypes, measured by Luminex, in *Sle1* and *Sle1*TLR-9$^{-/-}$ mouse culture supernatants collected after 96 hours of incubation. Cultures were left untreated, stimulated with R848, or stimulated with LPS. **E**, Expression of surface IgG (sIgG) (IgG1/IgG2a/IgG2b/IgG3) on freshly isolated B220+CD19+ splenocytes from *Sle1* and *Sle1*TLR-9$^{-/-}$ mice. **F** and **G**, TLR-7 expression and frequencies of splenic CD138+ plasma/plasmablasts (**F**) and CD11b+ dendritic cells (DCs) (**G**) in *Sle1* and *Sle1*TLR-9$^{-/-}$ mice. In **A**, **B**, and **D**, bars show the mean ± SEM from 2–3 independent experiments (n = 9–15 mice per group). Data were assessed by multiple *t*-tests, and statistical significance was corrected using the Holm-Sidak method. In **C**, **E**, **F**, and **G**, data are from 1 representative experiment with 8–10-week-old mice (n = 8 *Sle1* and 5 *Sle1*TLR-9$^{-/-}$ mice). Circles represent individual mice; horizontal lines and error bars show the mean ± SEM. Significance was determined by Student's *t*-test. * = $P < 0.05$; ** = $P < 0.01$; *** = $P < 0.001$; **** = $P < 0.0001$.

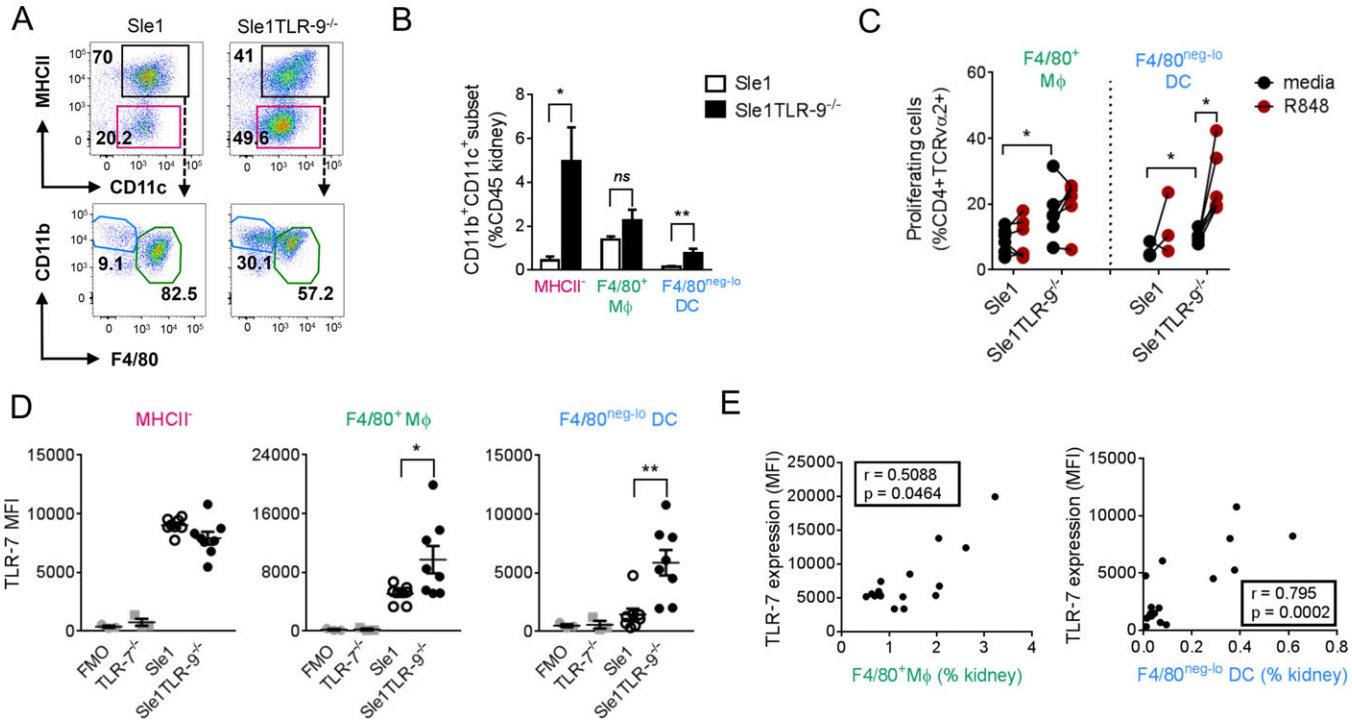

Figure 5. Infiltration of dendritic cells (DCs) with increased Toll-like receptor 7 (TLR-7) protein expression into *Sle1*TLR-9$^{-/-}$ mouse kidneys. **A**, Analysis of renal CD45+CD11b+Gr-1$^{-/low}$ subsets using antibodies to CD11c, major histocompatibility complex class II (MHCII), F4/80, and CD11b. The magenta boxed area includes the CD11c+MHCII− precursor population. The black boxed area includes the CD11c+MHCII+ cells. CD11c+MHCII+ cells were further subdivided into F4/80+ macrophages (Mϕ; green encircled area) and F4/80$^{-/low}$ DCs (blue encircled area). **B**, Cumulative frequencies of renal CD11b+Gr-1− subsets identified in **A** in *Sle1* and *Sle1*TLR-9$^{-/-}$ mice. Bars show the mean ± SEM. Data are from 3 independent cohorts of 4.5–6.5-month-old mice with a total of 9–16 mice per group. **C**, Proliferation of CD4+TCRvα2+ *Sle1*OT-II cells exposed to ovalbumin-pulsed F4/80+ macrophages or F4/80$^{-/low}$ DCs, with or without prior stimulation with R848. Circles represent cells sorted from an individual mouse (n = 6), except for *Sle1* F4/80$^{-/low}$ DCs that were pooled to a total of 3 samples due to low cell numbers. **D**, Analysis of TLR-7 protein expression, using flow cytometry, in the CD11b+Gr-1− subsets identified in **A** in *Sle1* and *Sle1*TLR-9$^{-/-}$ mice. Symbols represent individual samples; horizontal lines and error bars show the mean ± SEM. **E**, Correlation of TLR-7 expression in *Sle1* and *Sle1*TLR-9$^{-/-}$ mice with percentages of renal macrophage and DC infiltration. Data in **D** and **E** are from 3 independent experiments with a total of 8 mice (ages 5.7–6.4 months) per group. Each experiment was conducted with a TLR-7$^{-/-}$ and a fluorescence minus one (FMO) control (a total of 3 each). Parametric data were assessed by one-way analysis of variance (with Bonferroni adjustment for multiple comparisons) or Student's *t*-test, and nonparametric data were assessed by Kruskal-Wallis test (with Dunn's multiple comparison test) or Mann-Whitney test. Correlations were determined using Spearman's rank correlation for nonparametric data and Pearson's correlation for parametric data. * = $P < 0.05$; ** = $P < 0.01$. NS = not significant; MFI = median fluorescence intensity.

did not detect an increase in TLR-7 protein in B cells in young mice (Figure 4C). However, analyses of supernatants collected on day 4 revealed that *Sle1*TLR-9$^{-/-}$ mouse cultures produced significantly higher amounts of IgG upon stimulation with R848 or LPS (Figure 4D). Moreover, in the absence of any stimulation, *Sle1*TLR-9$^{-/-}$ B cells spontaneously released IgG2b and IgG3, in contrast to their *Sle1* counterparts (Figure 4D).

No differences were detected between *Sle1*TLR-9$^{-/-}$ mice and *Sle1* mice in IgM and IgGA production, suggesting an increase in IgG isotype switching (Supplementary Figure 4D). We thus stained freshly isolated mouse splenocytes with a cocktail of anti-IgG1/IgG2a/IgG2b/IgG3 antibodies and analyzed them by flow cytometry (gating strategy is shown in Supplementary Figure 4E). We confirmed that *Sle1*TLR-9$^{-/-}$ mouse B cells expressed significantly more surface IgG than their *Sle1* mouse counterparts (Figure 4E). Additionally, the frequencies of CD138+ plasma/plasmablast cells were increased and they expressed significantly higher TLR-7 protein levels in the absence of TLR-9 (Figure 4F and Supplementary Figure 4F). Extrafollicular plasmablast responses and antibody switching in lupus have been attributed to DCs (39). We detected increased frequencies of splenic CD11b+ DCs with higher TLR-7 expression in *Sle1*TLR-9$^{-/-}$ mice (Figure 4G). This early stage expansion of TLR-7–high DCs might play a role in the increase in CD138+ plasma/plasmablasts and IgG-switched B cells in *Sle1*TLR-9$^{-/-}$ mice.

Kidney disease in *Sle1*TLR-9$^{-/-}$ mice is characterized by infiltrating renal cDCs that overexpress TLR-7. To further understand kidney pathogenesis in *Sle1*TLR-9$^{-/-}$ mice, we characterized renal leukocyte infiltrates, using a similar flow cytometry strategy as previously described for *Sle1* mice overexpressing TLR-7 (*Sle1*Tg7) (15). The majority of infiltrating cells in *Sle1*TLR-9$^{-/-}$ mouse kidneys were CD11b+Gr-1$^{-/low}$ (Supplementary Figure 1G). These consisted of 3 CD11c+ populations: MHCII−, F4/80+ macrophages, and F4/80$^{-/low}$ DCs (Figures 5A and B). As in *Sle1*Tg7 mice, the proportions of MHCII− and F4/80$^{-/low}$ DCs were increased in the kidneys of *Sle1*TLR-9$^{-/-}$ mice compared to *Sle1* mice, while the proportions of macrophages did not change significantly (15) (Figure 5B).

We then assessed the ability of DCs to present antigen and induce T cell proliferation by purifying renal DCs, or macrophages as a control, and exposing them to ovalbumin before culturing with *Sle1*OT-II T cells (15). Unstimulated DCs from *Sle1*TLR-9$^{-/-}$ mouse kidneys induced more T cell proliferation than those from *Sle1* controls, which was enhanced with the TLR-7 ligand R848 (Figure 5C and Supplementary Figure 5A, available on the *Arthritis & Rheumatology* web site at http://onlinelibrary.wiley.com/doi/10.1002/art.40535/abstract). Renal macrophages did not show augmented T cell proliferation with R848, consistent with earlier data from bone-marrow derived and peritoneal macrophages (40). Both renal DCs and macrophages had increased TLR-7 protein expression in the absence of TLR-9, and the levels positively correlated with the percentage of infiltrating renal DCs and macrophages (Figures 5D and E). Additionally, TLR-7 expression was increased in TLR-9–deficient *Sle1* kidney Gr1^{intermediate} CD11b+ cells, but not in pDCs and B cells (Supplementary Figure 5B). We did not detect TLR-7 expression in kidney PMNs and T cells (data not shown). To assess whether the increases in TLR-7 occurred prior to the development of GN, we analyzed younger *Sle1*TLR-9$^{-/-}$ mice with less severe disease, as confirmed by splenic weight and a lack of significant CD45+ kidney infiltration (Supplementary Figure 5C). Expression of TLR-7 was increased in *Sle1*TLR-9$^{-/-}$ mouse kidney F4/80+ macrophages and F4/80$^{-/low}$ DCs, but not in MHCII− cells, similar to their older counterparts (Supplementary Figure 5D).

DISCUSSION

Over the last decade, multiple studies have supported the notion of a fundamental role of TLR-7 in SLE disease development; however, little progress has been made to elucidate the regulatory role of TLR-9 (7–10,12–14,27,31–34,41). Moreover, the lack of data from human studies has reduced enthusiasm for understanding the cellular and molecular roles in TLR-9–deficient mice. In the present study, we have shown for the first time that TLR-7 is increased at the protein level prior to disease onset in TLR-9–deficient *Sle1* mice. Our data also show that in B cells, TLR-9 maintains tolerance to RNA and RNA-associated antigens, prevents antibody switching and antibody production, and regulates B cell maturation. Thus, in the absence of TLR-9, there is an accumulation of TLR-7–reactive RNA/anti-RNA–associated ICs that can activate the increased TLR-7 in DCs and B cells (Figure 6). This essentially yields an identical kidney inflammation phenotype to that observed in *Sle1*Tg7 mice, which have a modest increase in TLR-7 expression (15).

We and others have proposed a multistep model of lupus pathogenesis whereby there is an initial loss of tolerance to self, which, together with an additional immune alteration, leads to the progression of severe disease (42–44). We propose that the loss of tolerance to RNA plays a key role in the transition to active disease. Surprisingly, anti-RNA antibodies have not been studied extensively, despite showing high specificity for SLE (28). However, autoantibodies to RNA-associated molecules, such as snRNP, Sm, SSA/Ro, and SSB/La, are well characterized, and the presence of anti-Sm antibodies is part of the immunologic criteria for SLE diagnosis (45).

BWR4, an anti-RNA antibody derived from (NZB × NZW)F_1 mice, forms ICs in vitro by binding RNA present in the tissue culture supernatant (37). These RNA-containing ICs then activate cells through a B cell receptor (BCR)– and TLR-7–dependent mechanism. We showed that *Sle1*TLR-9$^{-/-}$ mouse serum predominantly produces a cytoplasmic HEp-2 staining pattern, similar to the anti-RNA antibody BWR4 (37). The increase in the cytoplasmic HEp-2 staining pattern and/or increased anti-RNA antibody levels are common to the few TLR-9–deficient model systems that have been examined (8,9,14). Increased levels of RNA-associated autoantibodies, such as anti-Sm, U1 snRNP-1, PM/Scl-100, and/or anti–ribosomal P, were also observed in TLR-9$^{-/-}$ models that develop severe kidney disease (8–10). On the other hand, when TLR-9 was eliminated on a milder autoimmune background, such as *Sle1b*, there was no increase in anti-Sm/RNP IgG (31). This might have important implications for human SLE, since there is evidence that anti-Sm and anti-snRNP antibodies are present immediately preceding the manifestation of clinical symptoms (42).

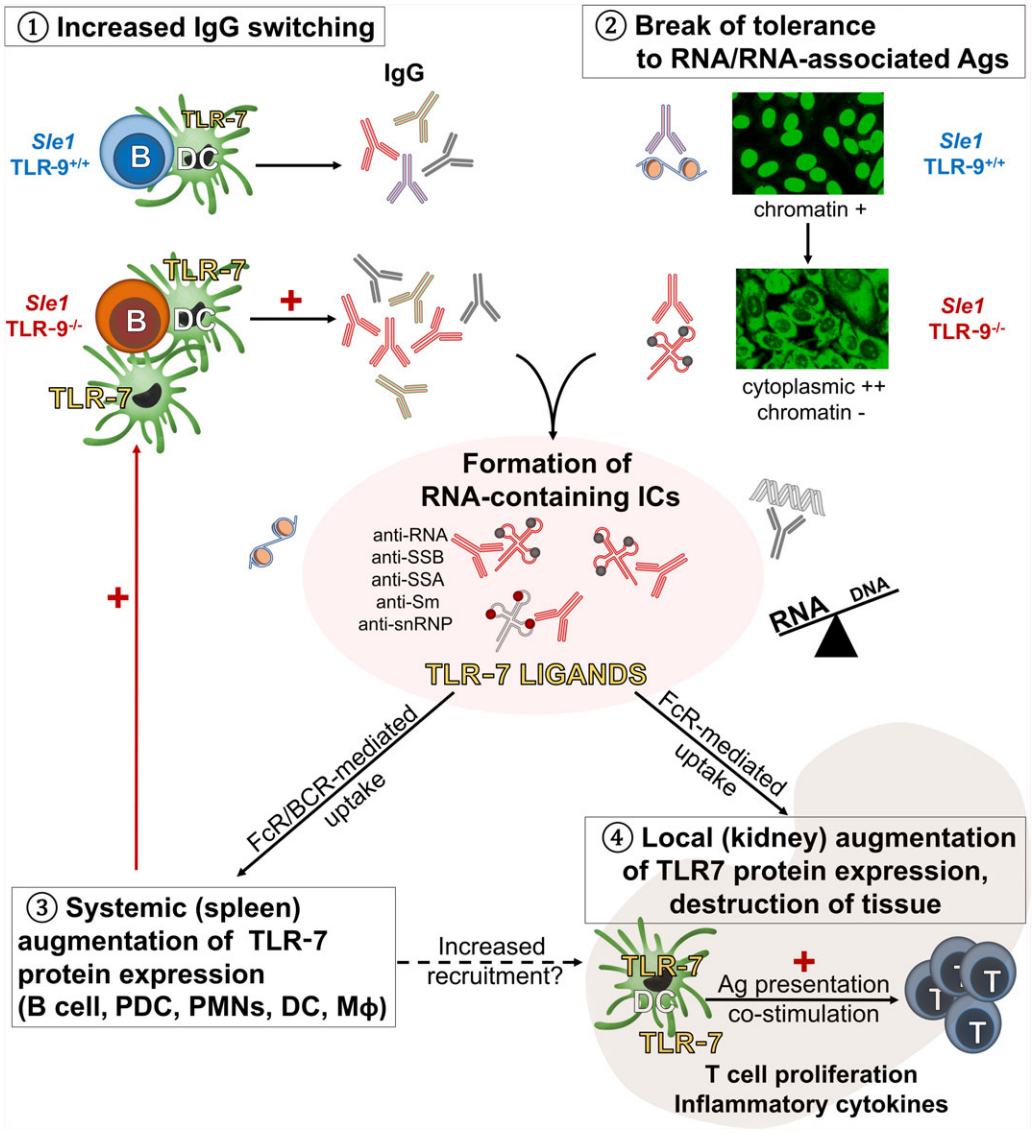

Figure 6. Schematic overview of the proposed mechanisms leading to severe disease in the absence of Toll-like receptor 9 (TLR-9). (1) B cells from prediseased *Sle1*TLR-9$^{-/-}$ mice are primed to produce more IgG-switched antibodies, most likely due to the presence of increased numbers of CD11b+ dendritic cells (DCs) with increased TLR-7 protein expression. (2) In the absence of TLR-9, the autoantibody repertoire shifts toward RNA/RNA-associated antigens (Ags), which leads to the generation of RNA-containing immune complexes (ICs). These complexes act as TLR-7 ligands through Fc receptor (FcR) and B cell receptor (BCR)–mediated uptake and induce TLR-7 protein expression through a positive feedback loop at the systemic (3) and organ (4) levels. A simultaneous increase in the levels of TLR-7 and its ligands leads to ongoing inflammation and tissue destruction through various mechanisms, including T cell proliferation and inflammatory cytokine generation. Anti-snRNP = anti–small nuclear RNP; pDCs = plasmacytoid DCs; PMNs = polymorphonuclear leukocytes; Mϕ = macrophages.

Aside from the autoantibody switch to RNA specificity, our data also suggest that the concomitant increase in TLR-7 plays a crucial role in the progression to end-organ damage. Since SLE serum and the TLR-7 agonist R848 have been shown to increase TLR-7 expression (19,46), the RNA-associated ICs in the circulation can increase TLR-7 through a positive feedback loop. This is supported by clinical data that shows a preferentially higher TLR-7 expression in SLE patients with an anti-RNA–associated antibody profile (47). Additionally, it has recently been shown that RNA-associated antibodies are more prone to form circulating ICs compared to antibodies to dsDNA (48). U1 RNA, which forms the U1 snRNP complex together with Sm and RNP proteins (49), is elevated in the circulation of SLE patients and correlates with disease activity (50).

Thus, while anti-RNA/RNA-associated antibodies might be less common than anti-dsDNA in SLE patients (28,49), they can form ICs more easily and enhance disease progression through TLR-7 binding and up-regulation (Figure 6).

In our earlier investigations we proposed that renal cDCs play a fundamental role in disease progression given their location, their increased inflammatory properties, and the correlation of their expansion with disease progression (15). Consistent with the findings of this study, *Sle1*TLR-9$^{-/-}$ renal cDCs have increased levels of TLR-7 protein and have an increased ability to stimulate T cells following TLR-7 ligation. Furthermore, TLR-7 in these populations correlated with leukocyte infiltration. Importantly, our analyses in younger mice indicated that the increase in renal cDCs occurred prior to significant leukocyte infiltration, suggesting that cDCs play a crucial role in disease progression.

In summary, we have identified multiple roles for the innate dsDNA receptor, TLR-9, in preventing the systemic inflammation and progression to severe disease in a lupus-prone mouse strain. In B cells, TLR-9 prevents excessive Ig production and the switch to RNA-reactive antibody production. In addition, TLR-9 controls TLR-7 at the protein level, most likely in an indirect manner by preventing TLR-7 ligands from being generated and by favoring DNA sensing over RNA sensing in the endosome (51). In the absence of TLR-9, the concomitant increase in the levels of TLR-7 and its ligands leads to ongoing inflammation and tissue destruction.

ACKNOWLEDGMENTS

We would like to thank Katja Lakota, PhD and Tinka Svec, MSc (The University Medical Centre Ljubljana, Ljubljana, Slovenia) for scoring of the HEp-2 slides and subsequent discussion. We thank the staff of the Flow Cytometry cores at Singapore Immunology Network and Institute of Molecular and Cell Biology, Agency for Science, Technology. and Research, for assistance with acquisition and sorting.

AUTHOR CONTRIBUTIONS

All authors were involved in drafting the article or revising it critically for important intellectual content, and all authors approved the final version to be published. Drs. Celhar and Fairhurst had full access to all of the data in the study and take responsibility for the integrity of the data and the accuracy of the data analysis.

Study conception and design. Celhar, Lim, Akira, Wakeland, Connolly, Fairhurst.

Acquisition of data. Celhar, Yasuga, Lee, Zharkova, Tripathi, Thornhill, Lu, Au, Lim, Thamboo.

Analysis and interpretation of data. Celhar, Au, Thamboo, Fairhurst.

REFERENCES

1. Akira S, Uematsu S, Takeuchi O. Pathogen recognition and innate immunity. Cell 2006;124:783–801.
2. Lee BL, Barton GM. Trafficking of endosomal Toll-like receptors. Trends Cell Biol 2014;24:360–9.
3. Mouchess ML, Arpaia N, Souza G, Barbalat R, Ewald SE, Lau L, et al. Transmembrane mutations in Toll-like receptor 9 bypass the requirement for ectodomain proteolysis and induce fatal inflammation. Immunity 2011;35:721–32.
4. Celhar T, Magalhaes R, Fairhurst AM. TLR7 and TLR9 in SLE: when sensing self goes wrong. Immunol Res 2012;53:58–77.
5. Marshak-Rothstein A. Toll-like receptors in systemic autoimmune disease. Nat Rev Immunol 2006;6:823–35.
6. Podolska MJ, Biermann MH, Maueroder C, Hahn J, Herrmann M. Inflammatory etiopathogenesis of systemic lupus erythematosus: an update. J Inflamm Res 2015;8:161–71.
7. Nickerson KM, Christensen SR, Shupe J, Kashgarian M, Kim D, Elkon K, et al. TLR9 regulates TLR7- and MyD88-dependent autoantibody production and disease in a murine model of lupus. J Immunol 2010;184:1840–8.
8. Christensen SR, Shupe J, Nickerson K, Kashgarian M, Flavell RA, Shlomchik MJ. Toll-like receptor 7 and TLR9 dictate autoantibody specificity and have opposing inflammatory and regulatory roles in a murine model of lupus. Immunity 2006;25:417–28.
9. Nickerson KM, Wang Y, Bastacky S, Shlomchik MJ. Toll-like receptor 9 suppresses lupus disease in Fas-sufficient MRL mice. PLoS One 2017;12:e0173471.
10. Santiago-Raber ML, Dunand-Sauthier I, Wu T, Li QZ, Uematsu S, Akira S, et al. Critical role of TLR7 in the acceleration of systemic lupus erythematosus in TLR9-deficient mice. J Autoimmun 2010;34:339–48.
11. Wu X, Peng SL. Toll-like receptor 9 signaling protects against murine lupus. Arthritis Rheum 2006;54:336–42.
12. Jackson SW, Scharping NE, Kolhatkar NS, Khim S, Schwartz MA, Li QZ, et al. Opposing impact of B cell-intrinsic TLR7 and TLR9 signals on autoantibody repertoire and systemic inflammation. J Immunol 2014;192:4525–32.
13. Yu P, Wellmann U, Kunder S, Quintanilla-Martinez L, Jennen L, Dear N, et al. Toll-like receptor 9-independent aggravation of glomerulonephritis in a novel model of SLE. Int Immunol 2006;18:1211–9.
14. Bossaller L, Christ A, Pelka K, Nundel K, Chiang PI, Pang C, et al. TLR9 deficiency leads to accelerated renal disease and myeloid lineage abnormalities in pristane-induced murine lupus. J Immunol 2016;197:1044–53.
15. Celhar T, Hopkins R, Thornhill SI, De Magalhaes R, Hwang SH, Lee HY, et al. RNA sensing by conventional dendritic cells is central to the development of lupus nephritis. Proc Natl Acad Sci U S A 2015;112:E6195–204.
16. Bourke E, Bosisio D, Golay J, Polentarutti N, Mantovani A. The toll-like receptor repertoire of human B lymphocytes: inducible and selective expression of TLR9 and TLR10 in normal and transformed cells. Blood 2003;102:956–63.
17. Miettinen M, Veckman V, Latvala S, Sareneva T, Matikainen S, Julkunen I. Live Lactobacillus rhamnosus and Streptococcus pyogenes differentially regulate Toll-like receptor (TLR) gene expression in human primary macrophages. J Leukoc Biol 2008; 84:1092–100.
18. Zarember KA, Godowski PJ. Tissue expression of human Toll-like receptors and differential regulation of Toll-like receptor mRNAs in leukocytes in response to microbes, their products, and cytokines. J Immunol 2002;168:554–61.
19. Garcia-Romo GS, Caielli S, Vega B, Connolly J, Allantaz F, Xu Z, et al. Netting neutrophils are major inducers of type I IFN production in pediatric systemic lupus erythematosus. Sci Transl Med 2011;3:73ra20.
20. Bernasconi NL, Onai N, Lanzavecchia A. A role for Toll-like receptors in acquired immunity: up-regulation of TLR9 by BCR

triggering in naive B cells and constitutive expression in memory B cells. Blood 2003;101:4500–4.
21. Roach JC, Glusman G, Rowen L, Kaur A, Purcell MK, Smith KD, et al. The evolution of vertebrate Toll-like receptors. Proc Natl Acad Sci U S A 2005;102:9577–82.
22. Plotz PH. The autoantibody repertoire: searching for order. Nat Rev Immunol 2003;3:73–8.
23. Morel L, Mohan C, Yu Y, Croker BP, Tian N, Deng A, et al. Functional dissection of systemic lupus erythematosus using congenic mouse strains. J Immunol 1997;158:6019–28.
24. Hemmi H, Takeuchi O, Kawai T, Kaisho T, Sato S, Sanjo H, et al. A Toll-like receptor recognizes bacterial DNA. Nature 2000;408:740–5.
25. Hemmi H, Kaisho T, Takeuchi O, Sato S, Sanjo H, Hoshino K, et al. Small anti-viral compounds activate immune cells via the TLR7 MyD88-dependent signaling pathway. Nat Immunol 2002; 3:196–200.
26. Weening JJ, D'Agati VD, Schwartz MM, Seshan SV, Alpers CE, Appel GB, et al, on behalf of the International Society of Nephrology and Renal Pathology Society Working Group on the Classification of Lupus Nephritis. The classification of glomerulonephritis in systemic lupus erythematosus revisited [published erratum appears in Kidney Int 2004;65:1132]. Kidney Int 2004; 65:521–30.
27. Fairhurst AM, Hwang SH, Wang A, Tian XH, Boudreaux C, Zhou XJ, et al. Yaa autoimmune phenotypes are conferred by overexpression of TLR7. Eur J Immunol 2008;38:1971–8.
28. Blanco F, Kalsi J, Isenberg DA. Analysis of antibodies to RNA in patients with systemic lupus erythematosus and other autoimmune rheumatic diseases. Clin Exp Immunol 1991;86:66–70.
29. Martin RM, Brady JL, Lew AM. The need for IgG2c specific antiserum when isotyping antibodies from C57BL/6 and NOD mice. J Immunol Methods 1998;212:187–92.
30. Wang A, Fairhurst AM, Tus K, Subramanian S, Liu Y, Lin F, et al. CXCR4/CXCL12 hyperexpression plays a pivotal role in the pathogenesis of lupus. J Immunol 2009;182:4448–58.
31. Soni C, Wong EB, Domeier PP, Khan TN, Satoh T, Akira S, et al. B cell-intrinsic TLR7 signaling is essential for the development of spontaneous germinal centers. J Immunol 2014;193: 4400–14.
32. Hwang SH, Lee H, Yamamoto M, Jones LA, Dayalan J, Hopkins R, et al. B cell TLR7 expression drives anti-RNA autoantibody production and exacerbates disease in systemic lupus erythematosus-prone mice. J Immunol 2012;189:5786–96.
33. Deane JA, Pisitkun P, Barrett RS, Feigenbaum L, Town T, Ward JM, et al. Control of toll-like receptor 7 expression is essential to restrict autoimmunity and dendritic cell proliferation. Immunity 2007;27:801–10.
34. Lartigue A, Courville P, Auquit I, Francois A, Arnoult C, Tron F, et al. Role of TLR9 in anti-nucleosome and anti-DNA antibody production in lpr mutation-induced murine lupus. J Immunol 2006;177:1349–54.
35. Zigon P, Lakota K, Cucnik S, Svec T, Ambrozic A, Sodin-Semrl S, et al. Comparison and evaluation of different methodologies and tests for detection of anti-dsDNA antibodies on 889 Slovenian patients' and blood donors' sera. Croat Med J 2011;52:694–702.
36. Ghirardello A, Villalta D, Morozzi G, Afeltra A, Galeazzi M, Gerli R, et al. Evaluation of current methods for the measurement of serum anti double-stranded DNA antibodies. Ann N Y Acad Sci 2007;1109:401–6.
37. Lau CM, Broughton C, Tabor AS, Akira S, Flavell RA, Mamula MJ, et al. RNA-associated autoantigens activate B cells by combined B cell antigen receptor/Toll-like receptor 7 engagement. J Exp Med 2005;202:1171–7.
38. Desnues B, Macedo AB, Roussel-Queval A, Bonnardel J, Henri S, Demaria O, et al. TLR8 on dendritic cells and TLR9 on B cells restrain TLR7-mediated spontaneous autoimmunity in C57BL/6 mice. Proc Natl Acad Sci U S A 2014;111:1497–502.
39. Teichmann LL, Ols ML, Kashgarian M, Reizis B, Kaplan DH, Shlomchik MJ. Dendritic cells in lupus are not required for activation of T and B cells but promote their expansion, resulting in tissue damage. Immunity 2010;33:967–78.
40. Celhar T, Pereira-Lopes S, Thornhill SI, Lee HY, Dhillon MK, Poidinger M, et al. TLR7 and TLR9 ligands regulate antigen presentation by macrophages. Int Immunol 2016;28:223–32.
41. Pisitkun P, Deane JA, Difilippantonio MJ, Tarasenko T, Satterthwaite AB, Bolland S. Autoreactive B cell responses to RNA-related antigens due to TLR7 gene duplication. Science 2006;312:1669–72.
42. Arbuckle MR, McClain MT, Rubertone MV, Scofield RH, Dennis GJ, James JA, et al. Development of autoantibodies before the clinical onset of systemic lupus erythematosus. N Engl J Med 2003;349:1526–33.
43. Fairhurst AM, Wandstrat AE, Wakeland EK. Systemic lupus erythematosus: multiple immunological phenotypes in a complex genetic disease. Adv Immunol 2006;92:1–69.
44. Kanta H, Mohan C. Three checkpoints in lupus development: central tolerance in adaptive immunity, peripheral amplification by innate immunity and end-organ inflammation. Genes Immun 2009;10:390–6.
45. Petri M, Orbai AM, Alarcón GS, Gordon C, Merrill JT, Fortin PR, et al. Derivation and validation of the Systemic Lupus International Collaborating Clinics classification criteria for systemic lupus erythematosus. Arthritis Rheum 2012;64:2677–86.
46. Marshall JD, Heeke DS, Gesner ML, Livingston B, Van Nest G. Negative regulation of TLR9-mediated IFN-α induction by a small-molecule, synthetic TLR7 ligand. J Leukoc Biol 2007;82: 497–508.
47. Chauhan SK, Singh VV, Rai R, Rai M, Rai G. Distinct autoantibody profiles in systemic lupus erythematosus patients are selectively associated with TLR7 and TLR9 upregulation. J Clin Immunol 2013;33:954–64.
48. Ahlin E, Mathsson L, Eloranta ML, Jonsdottir T, Gunnarsson I, Ronnblom L, et al. Autoantibodies associated with RNA are more enriched than anti-dsDNA antibodies in circulating immune complexes in SLE. Lupus 2012;21:586–95.
49. Migliorini P, Baldini C, Rocchi V, Bombardieri S. Anti-Sm and anti-RNP antibodies. Autoimmunity 2005;38:47–54.
50. Doedens JR, Jones WD, Hill K, Mason MJ, Gersuk VH, Mease PJ, et al. Blood-borne RNA correlates with disease activity and IFN-stimulated gene expression in systemic lupus erythematosus. J Immunol 2016;197:2854–63.
51. Fukui R, Saitoh S, Matsumoto F, Kozuka-Hata H, Oyama M, Tabeta K, et al. Unc93B1 biases Toll-like receptor responses to nucleic acid in dendritic cells toward DNA- but against RNA-sensing. J Exp Med 2009;206:1339–50.